

# Study on Flow Field Optimization of Flow Distribution Disk of Double-unloaded Groove Piston Pump

Yuning SONG\*

Yingkou Institute of Technology, Department of Mechanical and Power Engineering, Yingkou, Liaoning, 115014, China

\*Corresponding Author: Yuning SONG, E-mail: songyuning1230@163.com

## Abstract:

By referring to all kinds of research data and summarizing the analysis and research of various kinds of distribution disks, a new type of distribution disc with double V-shaped unloading slots is designed again. Then, the new designed disk is loaded into the piston pump by CFD software to simulate. Finally, through simulation, it is concluded that the width of the triangle slot of the distribution plate is about  $10^\circ$ , the slope angle is about  $12^\circ$ , and the diameter of the unloading hole is about 0.8mm. When the diameter of the perforated hole is about 1.5mm, the flow curve of the unloading hole is the smoother. Pressure shock and noise are also minimized at this time. Draw By improving the damping tank, the flow noise and cavitation change are smaller than before.

**Keywords:** Diskette; Double V discharge slot; CFD; Damping tank

## 1 Introduction

According to the working principle of the axial piston pump and we know that in axial piston pump with flow table for interactive oil distribution, the valve plate plays an important role, with the hydraulic pump using the working reliability and life of great influence<sup>[1-3]</sup>. Pressure drop is too suddenly, the commonly used method is to open a small slot or hole to solve the impact phenomenon, make the oil pressure effect will not be too fierce, so as to resolve this sudden shock. Oil flow state and the axial plunger pump overall efficiency of performance are important<sup>[7-9]</sup>.

Using three-dimensional modeling software SolidWorks on valve plate of 3 d modeling, and then use analytic software ANSYS in the process of its use is parsed, on its stress strain curve and deformation nephogram, through the finite element analysis software of the simulation results verify the valve plate can meet the requirements of actual working conditions.

## 2 Valve Disc Wear Mechanism

Plunger pump in the process of practical work, the workers often will not consciously to ignore in the valve plate with flow process of tiny pit phenomenon, but those tiny pit is caused by air pockets<sup>[10-12]</sup>, under the research scholar that Na Chenglie research, he found the little bubbles will not only cause tremendous

noise when burst, will flow on the plate cylinder piston cavity even cause pockmark. And also deduce the unit area of solid when the bubble burst, the specific algorithm can be calculated using the following formula of impulse to.

$$I = \sqrt{2dl\rho(p - p_0)}$$

Type:  $p_0$ —The pressure of air pockets in the air;  
 $l$ —Back into liquid liquid column length;  
 $d$ —Raced back to the trip air bubble diameter;

Thus, when the bubble burst or annihilation, cylinder wall or with above all can form the cavitation flow plate or hemp pit phenomenon, this phenomenon with the diameter of the bubble, bubble pressure and the length of the plunger are closely linked. Therefore, the high pressure small diameter of cavity also cannot be ignored.

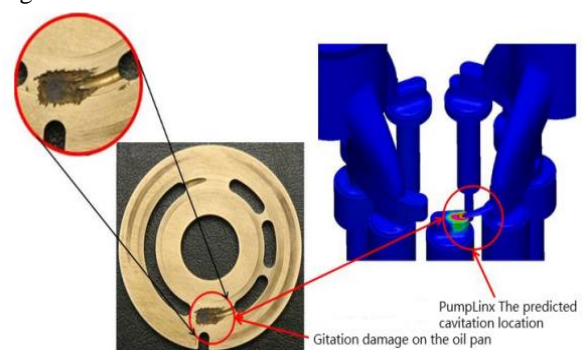


Figure 1 Validation of cavitation on the distribution plate

### 3 Different Types of Buffer Unloading Trough Analysis

Commonly used at home and abroad with more flow plate type structure though, but the basic sum up about three, as shown in figure 2, the common characteristics are above the waist type slot open certain buffer structure. When people begin to design the valve plate and did not expect to be above the waist type slot to open any shape, the most to the left of the shape as shown in figure 2, this one people usually call them the new structure of tradition. But, this kind of valve plate in the use of plunger pump, plunger pump can produce a lot of noise, and one more thing is, the flow of oil outlet presents the pulsation phenomenon. As a result, people started to analyze what causes of noise and ripple, after analysis found that the oil from the low pressure mode in the process of transition to the tank high waist type slot, because there is no preset buffer tank, oil instead of buffer room directly into high pressure cavity of the high and low pressure chamber of the oil pressure differs very big, go directly to is bound to cause ripple and noise, so going to find a way to improve, thus was born the figure 2 of the other two types of surge tank, triangle groove or u-shaped slot. This two kinds of buffer tank with the accumulation of years basically deflection to the use of triangular groove. But the study found that the triangle groove opening, although can play a buffer role, but the tip of the triangle groove parts easy to form stress concentration phenomenon, in order to solve the problem of stress concentration, open small round hole in the top of the triangle groove to solve the problem of stress. This and formed a new type of surge tank, hole groove type. Although this kind of valve plate can play a buffer role, but also can not guarantee the working rotation to the high-pressure plunger slot when rise of pressure and rotation to the trough of leakage pressure are equal, or easy to cause cavitation.

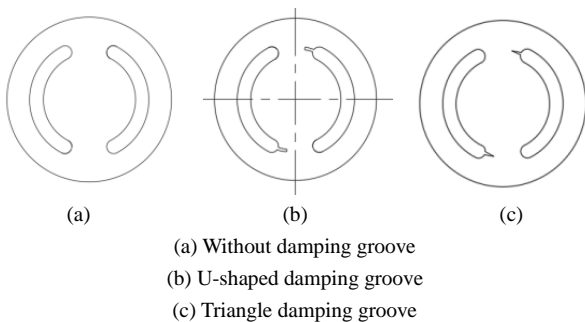


Figure 2 The structure type of the buffer tank

But for the new structure of triangular groove is easy to produce cavitation and noise phenomenon, in bad reading a lot of information about the direction of the valve plate, decided to change my single triangle groove opening to double triangular groove, and under the damping hole to open oil duct, its structure as shown in

figure as shown in 3.

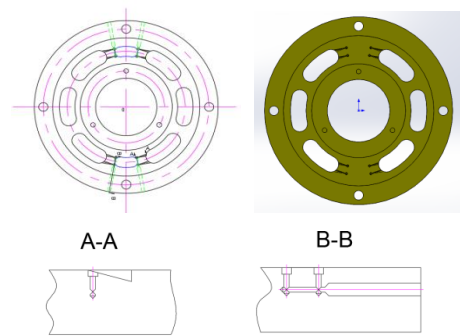


Figure3 Double buffered damping tank

### 4 Triangle Damping Groove Structure Design

In general, there must be a group in the actual work or combinations of several groups of data, makes the swashplate axial piston pump flow pressure in the process of impact on the smallest, minimum flow pulsation, the combination of minimum is noise data. However, due to such a complicated engineering problem, engineering practice and unable to provide detailed and accurate expression function, therefore, we once again on the basis of the original design, optimization design. The specific process as shown in figure 4:

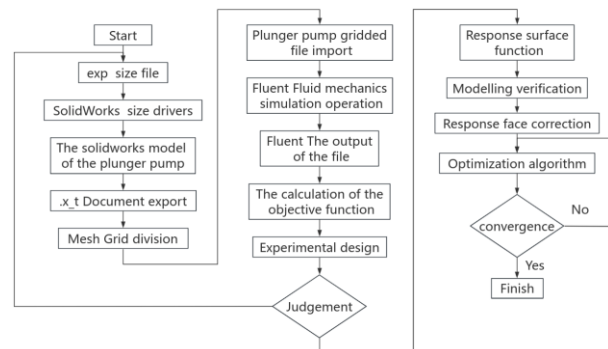


Figure 4 Buffer slot optimization design flow

### 5 Double Unloading Groove Plunger Pump with Flow Plate Flow Field Analysis

On the system of the internal flow field do certain simplified model, after I finish to simplify and according to the internal flow field of the actual operation situation made some basic assumptions, by assumption is as follows:

- (1) Assuming that the hydraulic oil for incompressible fluid;
- (2) Assume that the hydraulic oil for viscous Newtonian fluid;
- (3) Assumes the flow field of the system is steady;
- (4) Regardless of the fluid gravity;
- (5) Assume that no heat transfer within the hydraulic oil;

(6) Even within the system with the gas, assumes that the continuity equation is still available.

If you want to mathematical modeling on the flow field in the system, you first need to understand what kind of software for simulation analysis system internal flows. The second is to understand how to establish the mathematical model of you need. In general, our internal flow field of the whole system with powerful fluid parse function parses the fluent software. According to the previous hypothesis conditions, system of internal flow field as a fixed flow field. For fixed field flow phenomenon, usually uses a continuous equation and Bernoulli Reynolds averaged navier-stokes equations. In the algorithm, usually uses a simple algorithm and PISO algorithm. Here, we give a k - epsilon model equations of tensor form;

$$\frac{\partial \rho}{\partial t} + \frac{\partial}{\partial x_i}(\rho u_i) = 0 \quad (1)$$

$$\frac{\partial}{\partial t}(\overline{\rho u_i}) + \frac{\partial}{\partial x_j}(\overline{\rho u_i u_j}) = -\frac{\partial p}{\partial x_i} + \frac{\partial}{\partial x_j}(\mu \frac{\partial u_i}{\partial x_j} - \rho u_i u_j) + S_i \quad (2)$$

$$\frac{\partial}{\partial t}(\overline{\rho k}) + \frac{\partial}{\partial x_i}(\overline{\rho k u_i}) = \frac{\partial}{\partial x_j}((\mu + \frac{\mu_t}{\sigma_k}) \frac{\partial k}{\partial x_j}) + G_k + G_b - \rho \epsilon - Y_M + S_k \quad (3)$$

$$\frac{\partial}{\partial t}(\overline{\rho \epsilon}) + \frac{\partial}{\partial x_i}(\overline{\rho \epsilon u_i}) = \frac{\partial}{\partial x_j}((\mu + \frac{\mu_t}{\sigma_k}) \frac{\partial \epsilon}{\partial x_j}) + C_{1\epsilon} \frac{\epsilon}{k} (G_k + G_{3\epsilon} G_b) - G_{2\epsilon} \rho \frac{\epsilon^2}{k} + S_\epsilon \quad (4)$$

Type (1) as the continuity equation, the pattern is too all forms of Reynolds equation (2), type (3) the transport equation of turbulent kinetic energy k and epsilon type (4) is the turbulent kinetic energy dissipation rate of the transport equation.

Reynolds stress:

$$-\rho \overline{u_i u_j} = \mu_t (\frac{\partial u_i}{\partial x_j} + \frac{\partial u_j}{\partial x_i}) - \frac{2}{3} (\rho k + \mu_t \frac{\partial u_i}{\partial x_j}) \delta_{ij} \quad , \quad \text{Among}$$

them:  $\mu_t$  is the turbulent kinetic energy,  $\mu_t = \rho C_\mu \frac{k^2}{\epsilon}$ ;

$u_i$  is the average speed per hour;

$\delta_{ij}$  is the Kronecker delta;

$k$  is the urbulent kinetic energy,  $k = \frac{\overline{u_i u_i}}{2} = \frac{1}{2}(\overline{u^2 + v^2 + w^2})$ ;

$u_i \tilde{\cdot}$  is the fluctuating value;

$\epsilon$  is the turbulent dissipation rate,  $\epsilon = \frac{\mu}{\rho} \overline{(\frac{\partial u_i}{\partial x_k})(\frac{\partial u_i}{\partial x_k})}$ ;

$G_k$  is the due to the change of gradient generation rate, resulting in the turbulent kinetic energy k,

$$G_k = \mu_t (\frac{\partial u_i}{\partial x_j} + \frac{\partial u_j}{\partial x_i}) \frac{\partial u_i}{\partial x_j}$$

$G_b$  is caused by the buoyancy of turbulent kinetic energy k, for incompressible fluids,  $G_b=0$ ;

for compressible fluids,  $G_b = \beta g_i \frac{\mu_t}{Pr_t} \frac{\partial T}{\partial x_i}$ ;

$\beta$  is the thermal expansion coefficient,  $\beta = -\frac{1}{\rho} \frac{\partial \rho}{\partial T}$ ;

$P_{ri}$  is turbulent Prandtl number, in general,  $P_{ri}=0.85$ ,  $g_i$  is the gravitational acceleration in the direction of the  $i$ th component.

$Y_M$  representatives can be compressed fluctuations in the turbulent diffusion effect. For incompressible fluids,  $Y_M=0$ ; For compressible fluids,  $Y_M=2\rho\epsilon M_t^2$ ;  $M_t$  is turbulent Mach number,  $M_t = \sqrt{\frac{k}{a^2}} = \sqrt{\frac{k}{\gamma RT}}$ .

**Table1** High-pressure axial piston pump geometric model of the parameters

Parameter	Numerical	Parameter	Numerical
Pump Displacement Q	66cm <sup>3</sup> /R	Distribution Of Plug Diameter D	77mm
The Maximum Load Pressure P	35mp	Adjacent Piston Angle $\Theta_0$	40°
Cylinder Speed N	1500r/Min	The Plunger Hole Angle Range $\Psi_0$	25°
Plunger Number Z	Nine	The Initial Length Of Closed Volume $L_0$	22.1mm
Plunger Diameter D	19mm	Swash Plate Angle A	16°

$C_{1\epsilon}$ ,  $C_{2\epsilon}$ ,  $C_{3\epsilon}$  is empirical constan,  $\sigma_k$  and  $\sigma_\epsilon$  And the turbulent kinetic energy K and dissipation rate  $\epsilon$  corresponding Prandtl number,  $S_i$ 、 $S_k$ 、 $S_{\epsilon i}$  is user defined the source term. In the standard k - epsilon model, they respectively values as follows:  $C_{1\epsilon}=1.44$ ;  $C_{2\epsilon}=1.92$ ;  $C_{\mu}=0.09$ ;  $\sigma_k=1.0$ ;  $\sigma_\epsilon=1.3$ ; For  $C_{3\epsilon}$ , in compressible fluid, when the main flow direction and the gravity direction is parallel to each other,  $C_{3\epsilon}=1$ , Similarly, when they are perpendicular,  $C_{3\epsilon}=0$ .

Set up the new structure of four kinds of structure forms, respectively with traditional flow plate, with the new structure of V groove, the new structure of with u-shaped slot, and the new structure of double V groove.

Will be the new structure of four different structure forms, respectively with full port model (as shown in figure 5, figure 6) of the other components are combined, and then to compile analysis respectively, and the real-time monitoring for the export of oil, get export the flow curve of the oil, because did not take into account the oil leakage in the process of simulation, so it can monitor the flow of imported oil pump. Due to the different shape structure formed by the valve plate looks similar to the velocity field and pressure field distribution of change trend is basically the same. The difference is the size of the pressure value and speed.

In the process of practical work, each rotary plunger can produce 2 z flow pulsation in a week. Popular speaking, when a plunger cavity filled with oil absorption in the waist with the valve plate type when connected to oil tank, oil discharge cavity of the actual working

pressure generally higher plunger cavity oil pressure at this time, the poor and large load pressure). At this point, the discharge of oil waist type high pressure oil instantaneous slot will pressure into the plunger cavity, not only that, this part is instantaneous pressure into the plunger cavity of high pressure oil will flow through the flow pulsation in suction tank, this case the flow pulsation values are higher than the conventional pulse value of cases in other circumstances. Valve plate of oil outlet flow curve as shown in figure 11-14.

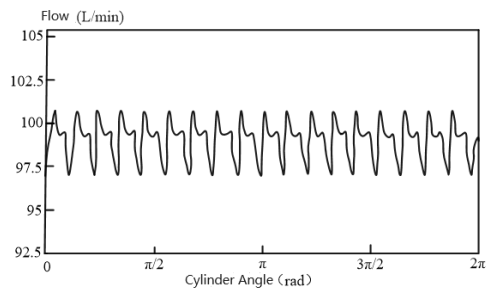


**Figure 11** Flow curve of traditional distribution plate

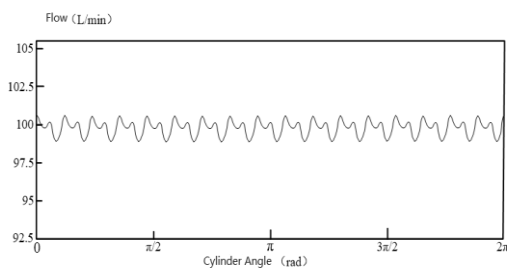


**Figure 12** Variation curve of U-slot platen

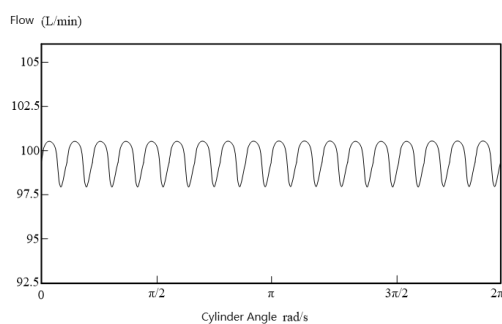


**Figure 13** Variation curve of V-slot platen

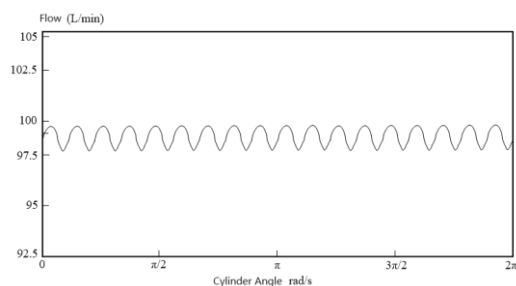


**Figure 14** Double V-groove distribution plate change curve

**Table 2** Flow pulsation of different shapes of the dispensing tray model

Model	$Q_{\max}$ L/Min	$Q_{\min}$ L/Min	$Q_{\text{ave}}$ L/Min	$\Delta$ %
Traditional	100.83	96.89	98.86	3.99
Single U	100.72	97.36	98.875	3.34
Single V	100.56	97.96	99.31	2.62
Double V	100.48	98.84	99.56	1.65

Through the analysis of 11-14, valve plate to join don't open any damping groove of flow fluctuation is bigger, and excessive is not smooth, a sharp peak, this situation is not conducive to the stability of pump, and because the peak is basically straight on straight down, cause the noise of the impact is bigger. Observed from figure 4.7 in turn down 4.10 can be found that the new structure of open u-shaped damping groove in the flow curve has slowed, but also in reducing volatility, but we want to make impact become smaller, to connect with flow plate and plunger cavity, smooth flow pulsation is becoming as much as possible, floating values become as small as possible, to reduce the noise, shock, we have designed the new structure of double "V" damping groove, on the one hand, V groove pointed mouth place from high pressure oil, can reduce half of the impact of noise can be reduced, and by observing the graph can be flow pulsation became more and more small, you may refer to specific parameter values are shown in table 2. Simulation proves that this design is helpful to improve the work efficiency of the pump noise, reduce the flow pulsation.

## 6 Process and Results Optimized by Using the Penalized Function Method

The span  $a$  and the width  $b$  of the triangle groove are defined as the design factors, the span of the high pressure side buffer groove of the distribution plate is recorded as  $a_1$  width as  $b_1$ , the span of the low pressure side buffer groove is recorded as  $a_2$  width as  $b_2$ , and the full factor method is used to obtain some arrangement and combination of the two factors. So-called full factor analysis is actually each factor in the experiment in accordance with the combination of combination results minus 1, combination of all factors are participated in not less than two independent repeated experiment, we put the formation of the full arrangement combination of new experimental factor method called full factor method. For example, factors  $m_1, m_2, m_3, m_4$  combined  $2k-1$  ( $k=4$ ), then we need to do 15 trials, in which the main effect is  $m_1, m_2, m_3, m_4$ , and the interaction effect is  $m_1 m_2, m_1 m_3, m_1 m_4, m_2 m_3, m_3 m_4, m_1 m_2 m_3, m_1 m_2 m_4, m_2 m_3 m_4, m_1 m_2 m_3 m_4$ , a total of 15 experiments.

In the test process, in order to avoid the problems of large calculation amount and low efficiency in the redesign process, the second-order response surface function is generally selected as the target performance approximate model of the inclined disc axial plunger

pump, as shown in Equation 5.

$$F = a_0 + \sum_{i=1}^n a_i X_i + \sum_{i=1}^n \sum_{j=1}^n b_{ij} X_i X_j \quad (5)$$

According to the structural characteristics of the pump and the processing and installation requirements, the width of the groove,  $a_1$ ,  $b_1$ ,  $a_2$ , and the width of the damping groove are  $a_{11}$ ,  $a_{12}$ ,  $a_{13}$ ,  $a_{14}$ , with a width,  $b_{11}$ ,  $b_{12}$ ,  $b_{13}$ , and  $a_{21}$ ,  $a_{22}$ ,  $b_{22}$ ,  $b_{23}$ ,  $b_{24}$ , as shown in Es. 6.

$$\begin{cases} 0 \leq a_{11} \leq 20^\circ \\ 0 \leq b_{11} \leq 5 \\ 0 \leq a_{21} \leq 20^\circ \\ 0 \leq b_{21} \leq 5 \end{cases}, \begin{cases} 0 \leq a_{12} \leq 20^\circ \\ 0 \leq b_{12} \leq 5 \\ 0 \leq a_{22} \leq 20^\circ \\ 0 \leq b_{22} \leq 5 \end{cases}, \begin{cases} 0 \leq a_{13} \leq 20^\circ \\ 0 \leq b_{13} \leq 5 \\ 0 \leq a_{23} \leq 20^\circ \\ 0 \leq b_{23} \leq 5 \end{cases}, \begin{cases} 0 \leq a_{14} \leq 20^\circ \\ 0 \leq b_{14} \leq 5 \\ 0 \leq a_{24} \leq 20^\circ \\ 0 \leq b_{24} \leq 5 \end{cases} \quad (6)$$

In order to use the constraint function expression, the optimization variable, the span angle  $a_1$ , the low-voltage damping groove width  $b_1$ , the angle  $a_2$ , and the high-pressure damping groove width  $b_2$  are expressed as constraint functions, as shown in Equation 7.

$$\begin{cases} g_1(X) = -x_1 \leq 0, & g_2(X) = 20 - x_1 \leq 0 \\ g_3(X) = -x_2 \leq 0, & g_4(X) = 5.0 - x_2 \leq 0 \\ g_5(X) = -x'_1 \leq 0, & g_6(X) = 20 - x'_1 \leq 0 \\ g_7(X) = -x'_2 \leq 0, & g_8(X) = 5.0 - x'_2 \leq 0 \end{cases} \quad (7)$$

The theoretical expression of the objective performance is shown in Equation 8,9 and 10.

$$\begin{cases} \Delta P_H = 10^{-3} \cdot [-0.108x_1^2 - 0.814x_2^2 - 12.455x_1 \cdot x_2 + 148.800x_1 + 5.914x_2 - 876.252] \\ Q_H = 10^{-3} \cdot [0.0896x_1^2 + 2.132x_2^2 - 13.81x_1x_2 - 9.633x_1 + 55.039x_2 + 197.98] \end{cases} \quad (8)$$

$$\begin{cases} \Delta P_L = 10^{-3} \cdot [-2.2x_1^2 - 1.8x_2^2 + 1.8x_1 \cdot x_2 + 73.2x_1 - 66.7x_2 - 618.8] \\ Q_L = 10^{-3} \cdot [20.0x_1^2 - 24.1x_2^2 + 10.4x_1 \cdot x_2 - 130.3x_1 + 188.3x_2 - 372.1] \end{cases} \quad (9)$$

$$R^2 = 1 - \frac{\sum_{j=1}^N [y_{rsm}(j) - \bar{y}(j)]^2}{\sum_{j=1}^N [y(j) - \bar{y}]^2} \quad (10)$$

Formula: it is the difference between the maximum pressure and the minimum pressure in the inner chamber with high pressure;  $Q_h$  refers to the flow flow in the simulation true value and the plane response value of the planned size; represents the simulation mean of each point in the design space;  $N$  represents the number of test points in the design space.  $R^2$  represents the determination coefficient, and the size of its value represents the difference between the reaction plane and the simulation plane value. If the value is within 0-1, when the value is 1, it means that the two are basically the same.

The function expression can basically reflect the performance of the objective function about the response of local structural changes, which can further replace

CFD simulation, and finally optimize and redesign the objective function, so as to improve the design efficiency of integration. Through the construction of the model and the CFD simulation test, the target performance function can be obtained, because there is a difference between the maximum value of inversion and pressure difference, so we introduce a new coefficient sum, so that the optimization values  $F_1$  and  $F_2$  of the overall structural design scheme can be obtained.

$$F_1 = \Delta P_H + \lambda_1 Q_H \quad (11)$$

$$F_2 = \Delta P_L + \lambda_2 Q_L \quad (12)$$

among:

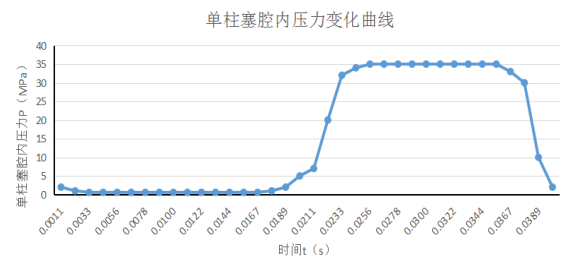
$$\lambda_1 = \frac{(\Delta P_H)_{\max} - (\Delta P_H)_{\min}}{(Q_H)_{\max} - (Q_H)_{\min}} \quad (13)$$

$$\lambda_2 = \frac{(\Delta P_L)_{\max} - (\Delta P_L)_{\min}}{(Q_L)_{\max} - (Q_L)_{\min}} \quad (14)$$

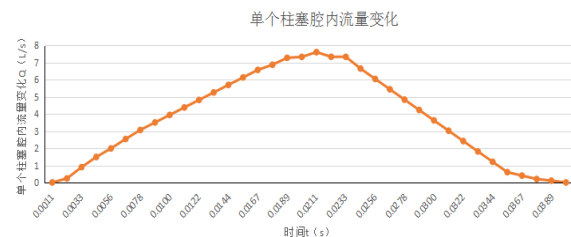
Here we choose the penalized function algorithm, and adopt the sorting method to solve the minimum value in Matlab. The design results are shown in Table 3.

**Table 3** Optimized results for manifolds

Optimiz e the variable	Buffer tank structure in the low-pressure zone				High-pressure zone buffer groove structure											
	$a_{11}$	$a_{12}$	$a_{13}$	$a_{14}$	$b_{11}$	$b_{12}$	$b_{13}$	$b_{14}$	$a_{21}$	$a_{22}$	$a_{23}$	$a_{24}$	$b_{21}$	$b_{22}$	$b_{23}$	$b_{24}$
Before optimiza tion																
postopti mality	10	3	3	10	3	3	11.365	2.561	2.31							



(a) Pressure change curve in a single plunger chamber



(b) Flow change curve in a single plunger cavity

**Figure 15** Damping groove optimization design cavity after the curves of pressure flow curve

The optimized triangle groove was modeled in 3 D with SolidWorks, and Fluent software was used to

simulate the relationship between pressure and flow in the plunger cavity. The simulation results are shown in Figure 15.

## 7 Conclusion

Through simulation with flow plate of triangle groove width open width is  $10^\circ$  or so, the best slope Angle is about  $12^\circ$ , the unloading hole at about 0.8 mm in diameter of holes, the unloading hole punched at about 1.5 mm in diameter of flow curve when compared with the smooth. At the same time, the impact pressure and noise also is the smallest. Is obtained by the improvement of damping groove, traffic noise and cavitation are becoming smaller than before.

**Fund project:** The Regional Joint Foundation plan of the Provincial Natural Science Foundation in 2022“Study on the characteristics of hydraulic frequency conversion vibrator for rotary valve distribution”(2022-YKLH-07);The Basic Scientific research Project of the Provincial Department of Education in 2023“Analysis of voltage control characteristics and transient temperature of electro-hydraulic transmission”(JYTMS20230063).

## References

- [1] Huang Hai-nan, He Xue-ming. Desalination in axial piston pump with flow plate structure optimization [J]. Pump Technology, 2018 (1):10-15.
- [2] Kong Xiang-chun, Nie Song-lin, Yin Fang-long. Water finale to the vibration characteristics of the plunger pump with flow are studied [J]. Hydraulics Pneumatics & Seals, 2018, 38(4): 28-32.
- [3] Chi Yu-rong, Yang Jun-ru. Simulation and Research on Flow Pulsation of Axial Piston Pump [J]. Machine Tool & Hydraulics, 2018, 46 (13): 138-143.
- [4] Hao Xi-yang, Wang Yu-lin. Study on Damping Groove Characteristics of Axial Plunger Pump [J]. Agricultural Equipment & Vehicle engineering, 2018, 56(7): 48-51.
- [5] Hou Wei, Nei Song-lin, Yin Fang-long. Optimization and Experimental Research for Silencing Groove Structure of Valve Plate in Water Hydraulic Piston Pump [J]. Chinese Hydraulics & Pneumatics, 2017 (8):8-13.
- [6] Diao Ying-xi. Four match flow axial piston pump with flow characteristic analysis and research [D]. Taiyuan technology university , 2017.
- [7] Cheng Jie. Axial piston motor with four match flow window flow theory and characteristic research [D]. Taiyuan university of science and technology, 2017.
- [8] Chi Yu-rong. The axial plunger pump output flow pulsation and the dynamic characteristics of the research [D]. Shandong university of science and technology, 2017.
- [9] Shi Xiang, Zhao Dong-biao. Structure Optimization of the Valve Plate of Aviation Piston Pump [J]. Machine Tool & Hydraulics, 2015, 43(22): 57-60.
- [10] ZHANG Yi, Gao You-shan. Simulation and Analysis of Axial Piston Pump with Four Distribution Windows [J]. Hydraulics Pneumatics & Seals, 2016, 3 6(3):18-21.
- [11] Shi Yan-ping, Zhang Yi. Simulation on Application of Axial Piston Pump with Parallel Dual Sucking and Discharging [J]. Hydraulics Pneumatics & Seals, 2016, 36(6):33-37.
- [12] Shi Ying-xun, Meng Guang-yao. Simulation Study on Effects of the Shape of Damping Groove on Cavitating Flow [J]. Chinese Hydraulics & Pneumatics, 2016(8): 108-111.
- [13] Chen Shuang-cheng. Based on the CFD desalination key techniques of axial piston pump [D]. Jiangnan university, 2016.
- [14] Yin Jin-feng. The structure of the axial piston pump damping groove optimization design [D]. Henan university of science and technology, 2015.
- [15] Bing XU, Ying-hui SUN, Jun-hui ZHANG, et al.. A New Design method for the transition Zone of Axial Piston pump Disc [J]. Journal of Zhejiang University-Science A(Applied Physics & Engineering), 2015,16(3):229-240.